Z. Kristallogr. 221 (2006) 246–251 / DOI 10.1524/zkri.2006.221.4.246

Crystal chemistry study of the solid solutions in the system La_2BaZnO_5–Eu_2BaZnO_5

Apuleyo Hernández-Pérez[I], Lauro Bucio[II], Alejandro Ibarra-Palos[I] and María Elena Villafuerte-Castrejón*,[I]

[I] Instituto de Investigaciones en Materiales, Universidad Nacional Autónoma de México, Cd. Universitaria, A.P. 70-360, 04510, México D.F.
[II] Instituto de Física, Universidad Nacional Autónoma de México, Cd. Universitaria A.P. 20-364, 01000, México D.F.

Received March 21, 2005; accepted September 1, 2005

Europium barium zinc oxides / Lanthanum barium zinc oxides / Solid solutions / Powder diffraction structure analysis / Rietveld refinement / X-ray diffraction

Abstract. In this work, a complete crystallochemical characterization of two solid solutions, which were founded in the binary end members system La_2BaZnO_5–Eu_2BaZnO_5, is reported. Both compounds belong to the family of mixed oxides with formula Ln_2BaMO_5 which presents interesting magnetic, electric and optical properties. Several works have been reported about this family of compounds with the same stoichiometry but with different structures depending on the M^{2+} coordination and rare earth content. Two solid solutions were obtained and characterized. Cell parameters, density measurements and solubility limits were determined for both solid solutions.

Structure refinements of Eu_2BaZnO_5, La_2BaZnO_5 and the two solid solution series were carried out by the Rietveld method. Both structures and their relationship were discussed.

Introduction

Mixed oxides with general formula RE_2BaMO_5 have been studied due to their interesting structural and physico-chemical properties [1]. When M^{2+} = Cu, they are formed as by-products or impurities called "green phases" during the synthesis of the $LnBa_2Cu_3O_{7-x}$ type superconductors [2].

This family presents four structural types characterized by different coordination polyhedra around the divalent transition metal [3].

These four groups can be described as follow: Type I: Isolated distorted square-pyramidal MO_5 units with space group *Pnma*, M = Cu, Zn, Co, Ni, RE = Sm, Eu, Gd, Tb, Dy, Y, Ho, Er, Tm, Yb, Lu; type II: infinite chains of MO_6 octahedra, space group *Immm*, M = Co, Ni, RE = Pr, Nd, Sm, Eu, Gd, Tb, Dy, Ho, Er, Tm, Yb, Lu; type III: isolated MO_4 square-planar units, the space group is *P4/mbm*, M = Cu, Pd, Pt, RE = La, Pr, Nd, Sm, Eu, Gd, Tb and type IV isolated MO_4 tetrahedra, space group *I4/mcm*, M = Zn and RE = La, Nd.

In this work, we studied the compounds of the binary system La_2BaZnO_5–Eu_2BaZnO_5. Both phases have different structural types: La_2BaZnO_5 has a tetragonal structure with space group *I4/mcm* and with isolated MO_4 tetrahedra [4]. Meanwhile, Eu_2BaZnO_5 is orthorhombic, space group *Pnma* and with isolated MO_5 square pyramidal units [5].

Although this family of compounds has been widely studied, not much work has been done in binary systems in which solid solutions have been formed [6]. Our mean interest is to study the structural change when different RE cations are introduced in the lattice in order to form solid solutions series in both sides of the binary system.

Wong-Ng, *et al.* report the Rietveld refinement results from synchrotron radiation and neutron diffraction data for BaR_2ZnO_5 (R=La, Nd, Dy, Ho, Er and Y), but not a solid solution series [7]. We have recently reported the $Eu_{1.8}La_{0.2}BaZnO_5$ structure [8].

Experimental

Sample preparation

The solid solutions series were prepared by solid state reaction. Starting materials were La_2O_3 (99.99%, Aldrich), Eu_2O_3 (99.99%, Aldrich), $BaCO_3$ (99.99%, Aldrich) and ZnO (99.99, Aldrich). Appropriated quantities of the reactants with 10 g total weight were mixed with acetone for at least 10 min in an agate mortar and pestle. Powders were heated in air, using tin oxide crucibles at 700 °C for few hours to expel CO_2, finally products of La_2BaZnO_5 with Eu^{3+} was fired at 1050 °C for a period of 2 to 5 days meanwhile compounds of Eu_2BaZnO_5 with La^{3+} were fired at 1200 °C for the same period of time. Since all compounds are easily hydrated, they were kept in desiccators.

X-ray diffraction analysis

Products were identified by X-ray powder diffraction with a Bruker axs D8 Advance, CuK_α radiation with secondary

* Correspondence author (e-mail: mevc@servidor.unam.mx)

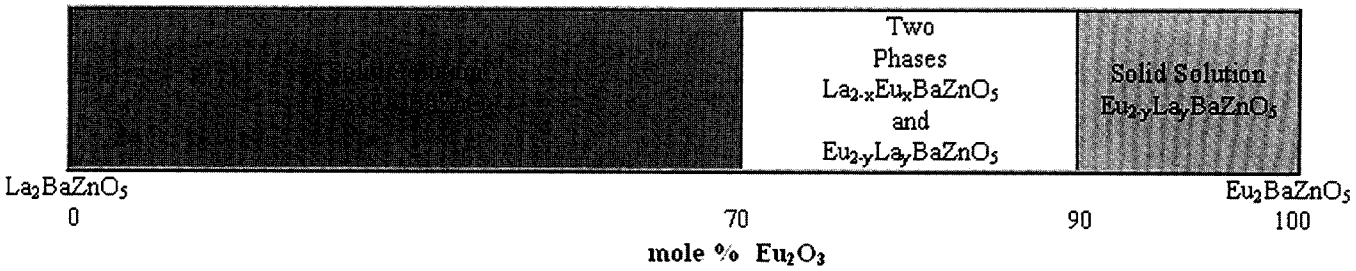

Fig. 1. Solubility range of the solid solutions and the range in which a mixture of the two phases appears.

graphite monocromator (35 kV, 30 mA), $\lambda = 1.5406$ Å. For accurate determination of the lattice parameters, a scan range 10°–110° 2θ, with 0.02° and 12 s as a count time per-step was used. DIFFRACT Release 2000, Eva V6.0 rev 0 program [9] was used to obtain well resolved powder lines. Structure refinements by the Rietveld method from X-ray powder diffraction data were carried out using the Fullprof program [10]. The employed profile was a pseudo-Voigt function. To determine the crystal structure, from powder diffraction data, the isostructural compounds Nd_2BaZnO_5 [11] and Y_2BaZnO_5 [12] were the starting model.

The density measurements were performed using specific gravity bottles with CCl_4 as displacement liquid.

Results and discussion

In the La_2BaZnO_5–Eu_2BaZnO_5 binary system, two solid solution series were synthesized and characterized by X-ray powder diffraction, Rietveld refinement and density measurements.

Figure 1 shows the solubility range of the solid solutions and the range in which a mixture of the two phases appears as function of La^{3+} and Eu^{3+} content. Figure 2 shows the X-ray diffraction patterns of $La_{2-x}Eu_xBaZnO_5$ solid solutions series as a function of x amount.

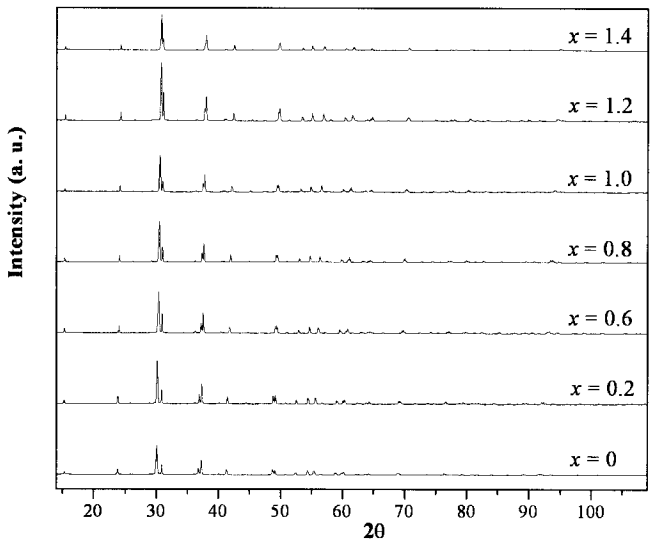

Fig. 2. X-ray powder diffraction pattern of $La_{2-x}Eu_xBaZnO_5$ ($x = 0$–1.4).

$La_{2-x}Eu_xBaZnO_5$ solid solution

La_2BaZnO_5 with Eu^{3+} forms an extensive range of solid solutions with formula: $La_{2-x}Eu_xBaZnO_5$ with $0 \leq x \leq 1.4$.

The proposed replacement mechanism of the solid solution formation is: $La^{3+} \leftrightarrow Eu^{3+}$, which was supported by density measurements and cell parameters evolution (Table 1).

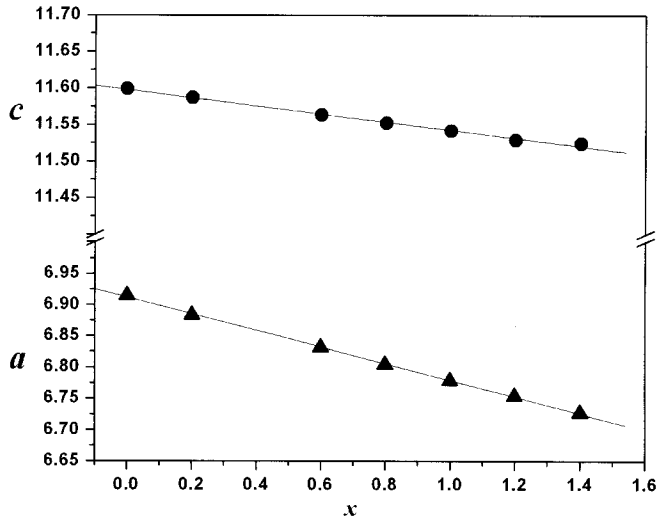

Fig. 3. Cell parameters as a function of x in $La_{2-x}Eu_xBaZnO_5$ solid solution. A linear fit for a and c are shown (R = 0.9997 and 0.99765, respectively).

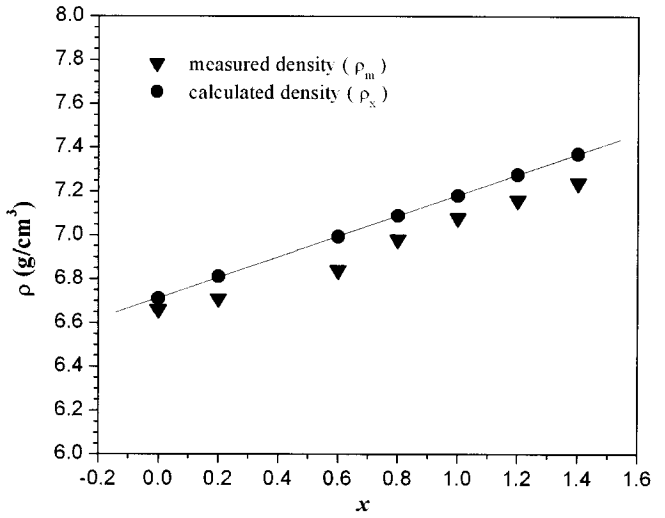

Fig. 4. Experimental and calculated density measurements as a function of x in $La_{2-x}Eu_xBaZnO_5$ solid solution. A linear fit for calculated density is shown (R = 0.99997).

Table 1. Cell parameters of $La_{2-x}Eu_xBaZnO_5$.

x	a (Å)	c (Å)	V (Å^3)	F.W. (g/mole)	ϱ_m (g/cm^3)[a]	ϱ_x (g/cm^3)
0.0	6.9148(1)	11.5989(1)	554.595(9)	560.53	6.66	6.7110(1)
0.2	6.8837(1)	11.5867(1)	549.034(4)	563.14	6.71	6.8106(1)
0.6	6.8315(1)	11.5637(1)	539.663(7)	568.36	6.84	6.9931(3)
0.8	6.8040(1)	11.5524(1)	534.808(5)	570.98	6.98	7.0891(1)
1.0	6.7789(1)	11.5416(1)	530.384(5)	573.59	7.08	7.1809(5)
1.2	6.7534(1)	11.5288(1)	525.809(8)	576.20	7.16	7.2763(3)
1.4	6.7271(1)	11.5238(2)	521.50(1)	578.81	7.24	7.3697(1)

a: error is 0.3%

Table 2. Reliability factors (%) for $La_{2-x}Eu_xBaZnO_5$ (not corrected for background).

x	R_{wp}	R_{exp}	R_{Bragg}	R_F	χ^2
0.0	11.1	6.63	5.88	5.06	2.79
0.2	10.5	5.89	6.32	5.52	3.19
0.6	11.2	5.97	6.70	5.18	3.55
0.8	10.4	6.20	5.58	4.78	2.79
1.0	10.3	6.64	4.84	4.35	2.39
1.2	11.9	5.58	6.94	5.05	4.57
1.4	12.9	6.94	5.16	5.60	3.48

Cell parameters are presented in Fig. 3. Both c and a decrease with Eu^{3+} content, but different slopes are observed in cell parameters plots showing that the contraction of c is smaller than a.

Experimental and calculated density values are shown in Fig. 4. Experimental data are well consistent with the calculated values for the proposed stoichiometric substitution. Experimental results are 1 to 3% lower than the calculated values for this solid solution replacement mechanism. This is a common effect observed when the density of a powder is measured using a displacement liquid and it is attributed to the difficulty in removing residual air on the surface of the particles. The important result is that the experimental data follow quite well the calculated data, indicating that the proposed mechanism of solid solution formation is correct.

For La_2BaZnO_5 and six compounds of its solid solution with Eu^{3+} ($La_{2-x}Eu_xBaZnO_5$, $x = 0.2$, 0.6, 0.8, 1.0, 1.2, 1.4) Rietveld refinements were carried out, the reliability factors of each refinement are listed in Table 2. The crystallographic data of these seven compounds are shown in Tables 3a and 3b, with the crystallographic positions and the thermal parameters for $La_{2-x}Eu_xBaZnO_5$ solid so-

Table 3a. Atomic positions for $La_{2-x}Eu_xBaZnO_5$ in *I4/mcm*.

Atom	site	x	y	z
La/Eu	8*h*	x_1	y_2	0.00
Ba	4*a*	0.0	0.0	0.25
Zn	4*b*	0.0	0.5	0.25
O1	4*c*	0.0	0.0	0.0
O2	16*l*	x_2	y_2	z_2

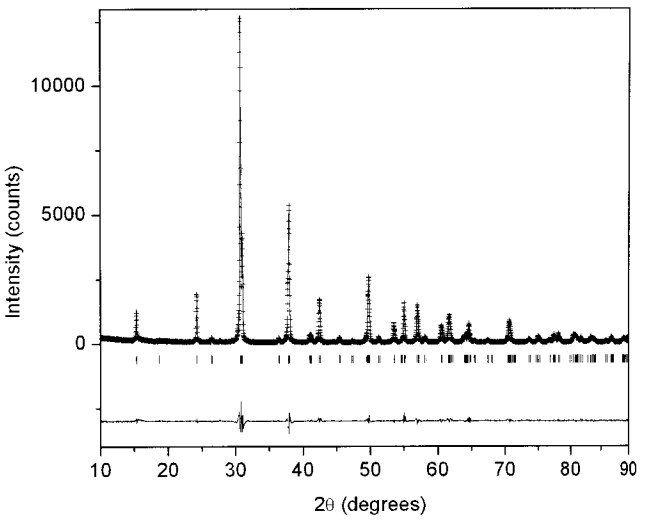

Fig. 5. Rietveld refinement results for $La_{0.6}Eu_{1.4}BaZnO_5$ ($x = 1.4$). Cross marks and continuous line represents the observed and calculated patterns respectively, the difference plot between them are shown below. Bragg positions are represented as vertical marks.

Table 3b. Atomic positions for $La_{2-x}Eu_xBaZnO_5$ corresponding to the parameters defined in Table 3a.

x	La/Eu		O_2			B_{iso} (Å^2)			
	x_1	y_1	x_2	y_2	z_2	La/Eu	Ba	Zn	O_1/O_2
0.0	0.1739(1)	0.6739(1)	0.3563(10)	0.8562(10)	0.1319(6)	0.62(3)	0.90(4)	0.60(8)	2.0(1)
0.2	0.1745(1)	0.6745(1)	0.3551(7)	0.8550(7)	0.1304(5)	0.25(2)	0.47(3)	0.57(7)	0.6(1)
0.6	0.1745(1)	0.6745(1)	0.3584(9)	0.8584(9)	0.1349(5)	0.34(3)	0.27(3)	0.28(7)	0.9(1)
0.8	0.1747(1)	0.6746(1)	0.3547(8)	0.8547(8)	0.1330(5)	0.15(2)	0.14(3)	0.11(6)	0.3(1)
1.0	0.1743(1)	0.6742(1)	0.3601(8)	0.8601(8)	0.1302(5)	0.41(2)	0.53(3)	0.25(6)	0.7(1)
1.2	0.1742(1)	0.6742(1)	0.3536(9)	0.8535(9)	0.1310(5)	0.54(2)	0.51(3)	0.49(7)	1.1(2)
1.4	0.1737(2)	0.6737(2)	0.3596(10)	0.8596(10)	0.1288(6)	0.86(3)	0.66(4)	0.87(9)	1.0(2)

lutions. Figure 5, is a Rietveld refinement plot for a representative member of the solid solution ($La_{0.6}Eu_{1.4}BaZnO_5$) which corresponds to the solubility limit.

$Eu_{2-y}La_yBaZnO_5$ solid solution

The solid solution on the opposite side of the binary system has a shorter solid solution limit, with the same replacement mechanism and following formula: $Eu_{2-y}La_yBaZnO_5$ with $0 \leq y \leq 0.2$. The corresponding cell parameters and density measurements are reported in Table 4. This solid solution has a smaller solubility range, two different compositions were obtained, $y = 0$ and 0.2; cell parameters are larger in $Eu_{1.8}La_{0.2}BaZnO_5$. As in the $La_{2-x}Eu_xBaZnO_5$ solid solutions, density measurements are in agreement with the proposed solid solution formation mechanism in which a stoichiometric substitution of the La^{3+} for Eu^{3+} occurs. The crystallographic positions for $Eu_{2-y}La_yBaZnO_5$ and the reliability factors for the corresponding Rietveld refinements are shown in Table 5.

Structural description of tetragonal system $La_{2-x}Eu_xBaZnO_5$ ($0 \leq x \leq 1.4$)

The structure (Fig. 6), is built up by La/EuO_8 bicapped trigonal prisms in alternative layers of La/Eu, ZnO_4 tetrahedra and BaO_{10} bicapped tetragonal antiprism. The symmetry is described by the space group *I4/mcm*, in which lanthanum ions with partial substitution of Eu^{3+} occupy 8*h* sites at the center of the bicapped trigonal prisms formed by O(1) and O(2) oxygens. The body of the trigonal prism is formed by O(2) while O(1), located at the origin of the unit cell, complete the two vertexes of the bicapped prism. The effect of Eu^{3+} substitution in the

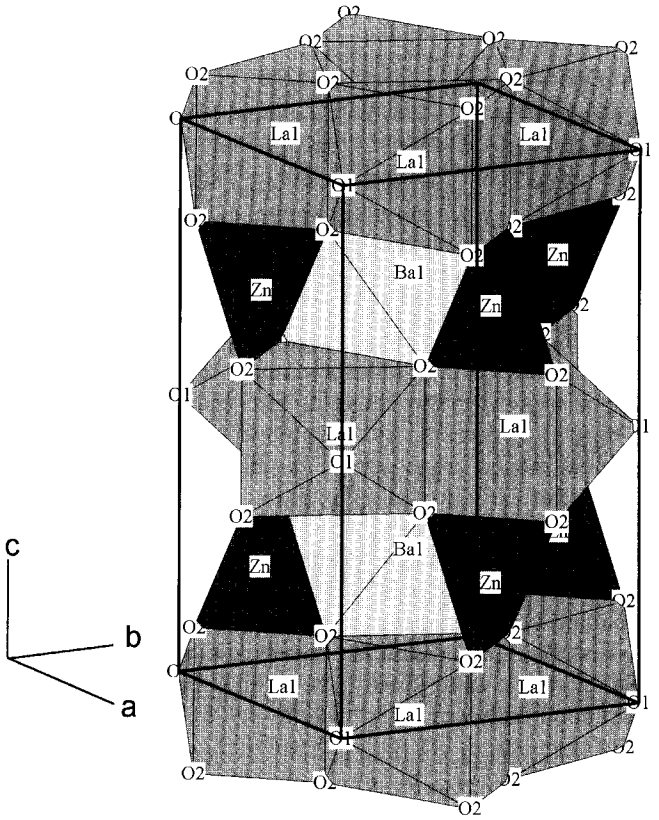

Fig. 6. $La_{2-x}Eu_xBaZnO_5$ structure.

structure increasing of x values, is reflected in the decrease of a parameter (Fig. 3). Bond distances (La/Eu)–O(1) become from 2.555 Å ($x = 0$) to 2.487 Å ($x = 1.4$), Table 6, so O(1) corners of the bicapped prism become closer with

Table 4. Cell parameters for $Eu_{2-y}La_yBaZnO_5$.

y	a (Å)	b (Å)	c (Å)	V (Å^3)	F.W. (g/mole)	ϱ_m (g/cm^3)[a]	ϱ_x (g/cm^3)
0.0	7.17634(8)	12.5317(1)	5.78936(7)	520.65(1)	586.627	7.32	7.4817(1)
0.2	7.1952(1)	12.5720(2)	5.8035(1)	524.97(1)	584.04	7.27	7.3871(1)

a: error is 0.3%

Table 5. Atomic positions for $Eu_{2-y}La_yBaZnO_5$ in *Pbmn*, and reliability factors (%) not corrected for background.

		Eu_2BaZnO_5 ($y = 0$)				$Eu_{1.8}La_{0.2}BaZnO_5$ ($y = 0.2$)			
Atom	site	x	y	z	B_{iso}	x	y	z	B_{iso}
Eu1	4*c*	0.1182(3)	0.2928(1)	0.25	0.28(2)	0.1160(3)	0.2909(1)	0.25	0.24(4)
Eu2	4*c*	0.3974(2)	0.0739(1)	0.25	0.28(2)	0.3977(2)	0.0744(1)	0.25	0.08(4)
Ba	4*c*	0.9251(2)	0.9001(1)	0.25	1.04(3)	0.9267(3)	0.9012(1)	0.25	0.11(4)
Zn	4*c*	0.6906(5)	0.6466(3)	0.25	0.9(1)	0.6848(5)	0.6501(3)	0.25	1.1(1)
O1	8*d*	0.166(1)	0.432(1)	0.013(2)	0.4(2)	0.157(1)	0.422(1)	0.013(2)	1.0(2)
O2	8*d*	0.376(2)	0.2229(9)	0.511(2)	0.4(2)	0.362(2)	0.2320(9)	0.511(2)	1.0(2)
O3	4*c*	0.077(2)	0.112(1)	0.25	0.4(2)	0.087(2)	0.100(1)	0.25	1.0(2)
Reliability factors (%)									
R_{wp}			10.9				11.7		
R_{exp}			4.74				7.03		
R_{Bragg}			7.90				7.05		
R_F			5.19				4.65		
χ^2			5.25				2.78		

Table 6. Atomic distances for $La_{2-x}Eu_xBaZnO_5$.

	$x = 0$	$x = 0.2$	$x = 0.6$	$x = 0.8$	$x = 1.0$	$x = 1.2$	$x = 1.4$
(La1/Eu1)–(O1) × 2	2.555(1)	2.542(1)	2.523(1)	2.513(1)	2.504(1)	2.495(1)	2.487(1)
(La1/Eu1)–(O2) × 2	2.349(7)	2.318(5)	2.364(6)	2.316(6)	2.331(6)	2.284(6)	2.309(7)
(La1/Eu1)–(O2) × 4	2.685(7)	2.675(5)	2.673(6)	2.672(6)	2.617(6)	2.646(6)	2.592(7)
(Ba)–(O1) × 2	2.900(3)	2.897(3)	2.891(3)	2.888(3)	2.885(3)	2.882(3)	2.881(5)
(Ba)–(O2) × 8	2.989(7)	2.982(5)	2.950(6)	2.937(6)	2.961(6)	2.926(6)	2.949(7)
(Zn)–(O2) × 4	1.963(7)	1.978(5)	1.909(6)	1.945(6)	1.926(6)	1.959(6)	1.933(7)

the x content. In its turn, because of (La/Eu)–O(2) bond distances have not significant change, the body of the bi-capped trigonal prism keeps its size and is only distorted in their O(1) corners. As a consequence of this distortion, different slopes are observed in cell parameters plots as function of Eu^{3+} content (Fig. 3).

Concerning the BaO_{10} polyhedra, they are linked sharing their O(1) vertexes forming –Ba–O(1)–Ba–O(1)– chains along the c-axis. For these polyhedra the corresponding bond distances are showed in Table 6. The variation of Ba–O(1) distances slightly diminish with x content as well c-axis. Finally, Zn is in a regular tetrahedron with bond distances from 1.909 to 1.978 Å (Table 6).

Structural description of orthorhombic system $Eu_{2-y}La_yBaZnO_5$ ($0 \leq y \leq 0.2$)

In the orthorhombic structure (Fig. 7), space group *Pbnm*, three different coordination polyhedra are present: Ba^{2+} occupy distorted tricapped quadrangular prisms; Zn^{2+} ions are in distorted square-based pyramids ZnO_5, whilst Eu^{3+} are in two non equivalent distorted monocapped trigonal prisms, one of them completely occupied by Eu^{3+} ions coordinated with seven oxygens, and the other with partially substituted by the La^{3+} ions introduced in the lattice. In monocapped trigonal prisms, the trigonal prism body is formed by O(2) and O(1), while O(3) completes the vertex of the monocapped prism. The resultant polyhedron is irregular with a variation in the bond distances Eu/La–O (Table 7). The prisms form chains joined by their edges alternating the site of Eu(1) and Eu/La(2), waving along the b-axis. This structure, in comparison to that already described, does not form layers. The BaO_{11} polyhedra are sharing their faces forming chains along the c-axis, which undulate in b-axis direction. In its turn these chains are linked together by sharing O(2) vertexes.

Table 7. Atomic distances for $Eu_{2-y}La_yBaZnO_5$.

	$y = 0$	$y = 0.2$
(Eu1)–(O1) × 2	2.25(1)	2.27(1)
(Eu1)–(O2) × 2	2.54(1)	2.37(1)
(Eu1)–(O2) × 2	2.23(1)	2.39(1)
(Eu1)–(O3)	2.28(1)	2.40(2)
(Eu2/La)–(O1) × 2	2.45(1)	2.30(1)
(Eu2/La)–(O1) × 2	2.28(1)	2.47(1)
(Eu2/La)–(O2) × 2	2.41(1)	2.42(1)
(Eu2/La)–(O3)	2.34(2)	2.25(2)
(Ba1)–(O1) × 2	3.19(1)	3.24(1)
(Ba1)–(O1) × 2	3.26(1)	3.38(1)
(Ba1)–(O2) × 2	3.04(1)	2.96(1)
(Ba1)–(O2) × 2	2.99(1)	3.06(1)
(Ba1)–(O3) × 2	2.898(1)	2.904(7)
(Ba1)–(O3)	2.86(1)	2.77(2)
(Zn)–(O1) × 2	2.08(1)	2.00(1)
(Zn)–(O2) × 2	2.19(1)	2.15(1)
(Zn)–(O3)	1.97(2)	2.05(2)

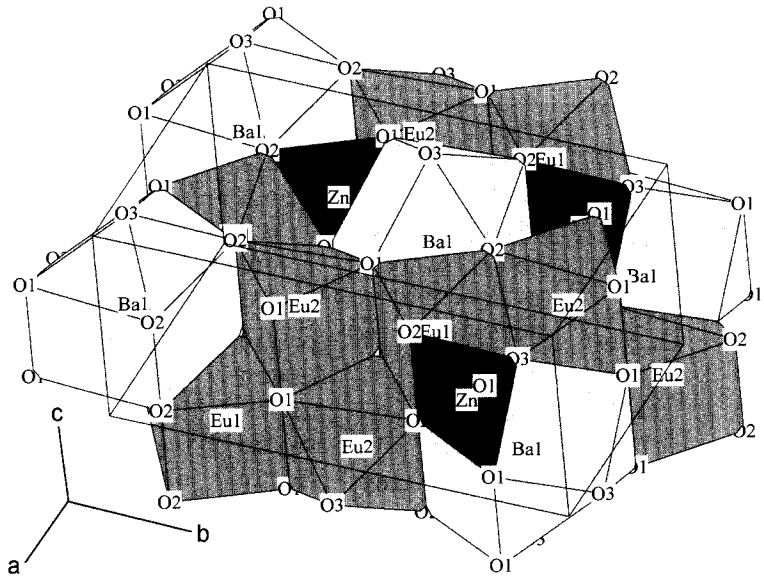

Fig. 7. $Eu_{2-y}La_yBaZnO_5$ structure.

The *relationship between both structures* can be summarized as follows:

In the tetragonal $La_{2-x}Eu_xBaZnO_5$ ($0 \leq x \leq 1.4$), as the Eu^{3+} increased the La/EuO_8 polyhedra size decrease, that can explains the different coordination number Eu/LaO_7 in the orthorhombic $Eu_{2-y}La_yBaZnO_5$ ($0 \leq y \leq 0.2$) structure as well as the decrease in the *c* cell parameter. The coordination of Zn^{2+} in the ZnO_5 polyhedron in the orthorhombic $Eu_{2-y}La_yBaZnO_5$ ($0 \leq y \leq 0.2$) is unusual in oxides. O(3) is both vertex of the polyhedra ZnO_5 and the monocapped trigonal polyhedra Eu/LaO_7. When La^{3+} amount is increase, the bond distance Zn–O(3) of the square-based pyramid increase along *c* axis, so in the tetragonal $La_{2-x}Eu_xBaZnO_5$ ($0 \leq x \leq 1.4$), became a ZnO_4 tetrahedron. The same effect is observed in Ba^{2+} polyhedra: In the orthorhombic structure is BaO_{11} decreasing the size with the increase of La^{3+} until change the coordination to BaO_{10} in the tetragonal structure. Smaller polyhedra cause the *b* cell parameter decrease, so with the increase of La^{3+} amount *b* becomes similar to *a* and *c* becomes longer, resulting in a tetragonal $La_{2-x}Eu_xBaZnO_5$ ($0 \leq x \leq 1.4$), with bicapped trigonal planes of La^{3+}.

Acknowledgment. We thank for the financial support extended by DGAPA, UNAM, PAPIIT No IN103603 and IN113814/15.

References

[1] Burdett, J. K.; Mitchell, J. F.: Crucial Interplay of Orbital and Cation-Anion Interactions in the Solid State: Distortions of NiO_6 Octahedra in $BaNiLn_2O_5$ Oxides. J. Am. Chem. Soc. **112** (1990) 6571–6579.

[2] Lavat, A. E.; Baran, E. J.; Sáez-Puche, R.; Salinas-Sánchez, A.; Martín-Llorente, M. J.: Infrared spectroscopic characterization of mixed oxides of the type $Ln_2BaM^{II}O_5$ (M = Co, Ni, Cu, Zn). Vibrational Spectroscopy **3** (1992) 290–298.

[3] Sáez-Puche, R.; Hernández-Velazco.: Structural relationships and Magnetic Behaviour in R_2BaMO_5 Oxides (R=Rare Earth; M = Co, Ni and Cu). J. Adv. Mater. Res. **1–2** (1994) 65–82.

[4] Sáez-Puche, R.; Coronado, J. M.; Otero-Díaz, C. L.; Martín Llorente, J. M.: Structural change and magnetic properties of $Y_2BaNi_{1-x}Zn_xO_5$ oxides. J. Solid State Chem. **93** (1991) 461–468.

[5] Kaduk, J. A.; Wong-Ng, W.; Greenwood, W.; Dillingham, J.; Toby, B. H.: Crystal structures and reference powder patterns of BaR_2ZnO_5 (R = La, Nd, Sm, Eu, Gd, Dy, Ho, Y, Er and Tm). J. Res. Natl. Inst. Stand. Technol. **104(2)** (1999) 147–171.

[6] Taibi, M.; Aride, J.; Antic-Fidancev, E.; Lemaitre-Blaise, M.; Porcher, P.: Crystal Field Parametres of Eu^{3+} and Nd^{3+} in Ln_2BaZnO_5. Phys. Stat. Sol. (a) **115** (1989) 523–531.

[7] Wong-Ng, W.; Toby, B.; Greenwood, W.: Crystallographic studies of BaR_2ZnO_5 (R = La, Nd, Dy, Ho, Er and Y). Powder Diffraction **13** (1998) 144–151.

[8] Hernández-Pérez, A.; Villafuerte-Castrejón, M. E.; Bucio, L.: $Eu_{1.8}La_{0.2}BaZnO_5$: a Rietveld Refinement Using X-ray Powder Diffraction. Acta Cryst. E**61** (2005) i23–i25.

[9] Siemens DIFFRAC/AT. Version 3.2. Siemens Analytical X-Ray Instruments Inc., Madison, Wisconsin, USA, (1993).

[10] Rodríguez-Carvajal, J.: Fullprof: A program for Rietveld refinement and pattern matching analysis. Abstracts of the Satellite Meeting of the 15th Congress of the IUCr. Toulouse, France. (1990) 127.

[11] Michel, C.; Er-Rakho L.; Raveau B.: Une nouvelle famille structurale: Les Oxydes $Ln_{4-2x}Ba_{2+2x}Zn_{2-x}O_{10-2x}$ (*Ln* = La, Nd). J. Solid State Chem. **42** (1982) 176–182.

[12] Michel, C.; Raveau, B.: Ln_2BaZnO_5 and $Ln_2BaZn_{1-x}Cu_xO_5$: A series of Zinc Oxides with Zinc in a Pyramidal Coordination. J. Solid State Chem. **49** (1983) 150–156.